Atherosclerosis 324 (2021) 18–26

Contents lists available at ScienceDirect

Atherosclerosis

journal homepage: www.elsevier.com/locate/atherosclerosis

Genotype-phenotype correlation in pseudoxanthoma elasticum

Jonas W. Bartstra [a,1], Sara Risseeuw [b,1], Pim A. de Jong [a], Bram van Os [a], Lianne Kalsbeek [a], Chris Mol [a], Annette F. Baas [c], Shana Verschuere [d], Olivier Vanakker [d], Ralph J. Florijn [e], Jeroen Hendrikse [a], Willem Mali [a], Saskia Imhof [b], Jeannette Ossewaarde-van Norel [b], Redmer van Leeuwen [b,2], Wilko Spiering [f,*,2]

[a] Department of Radiology, University Medical Center Utrecht, Utrecht University, the Netherlands
[b] Department of Ophthalmology, University Medical Center Utrecht, Utrecht University, the Netherlands
[c] Department of Genetics, University Medical Center Utrecht, Utrecht, the Netherlands
[d] Center for Medical Genetics, Ghent University Hospital, Ghent, Belgium
[e] Department of Clinical Genetics, Academic Medical Center, Amsterdam, the Netherlands
[f] Department of Vascular Medicine, University Medical Center Utrecht, Utrecht University, the Netherlands

ARTICLE INFO

Keywords:
Pseudoxanthoma elasticum
Arterial calcification
Peripheral arterial disease
ABCC6
Genotype-phenotype
Choroidal neovascularization

ABSTRACT

Background and aims: Pseudoxanthoma elasticum (PXE) is caused by variants in the *ABCC6* gene. It results in calcification in the skin, peripheral arteries and the eyes, but has considerable phenotypic variability. We investigated the association between the *ABCC6* genotype and calcification and clinical phenotypes in these different organs.

Methods: ABCC6 sequencing was performed in 289 PXE patients. Genotypes were grouped as two truncating, mixed, or two non-truncating variants. Arterial calcification mass was quantified on whole body, low dose CT scans; and peripheral arterial disease was measured with the ankle brachial index after treadmill test. The presence of pseudoxanthoma in the skin was systematically scored. Ophthalmological phenotypes were the length of angioid streaks as a measure of Bruchs membrane calcification, the presence of choroidal neovascularizations, severity of macular atrophy and visual acuity. Regression models were built to test the age and sex adjusted genotype-phenotype association.

Results: 158 patients (median age 51 years) had two truncating variants, 96 (median age 54 years) a mixed genotype, 18 (median age 47 years) had two non-truncating variants. The mixed genotype was associated with lower peripheral (β: 0.39, 95%CI:-0.62;-0.17) and total (β: 0.28, 95%CI:-0.47;-0.10) arterial calcification mass scores, and lower prevalence of choroidal neovascularizations (OR: 0.41 95%CI:0.20; 0.83) compared to two truncating variants. No association with pseudoxanthomas was found.

Conclusions: PXE patients with a mixed genotype have less severe arterial and ophthalmological phenotypes than patients with two truncating variants in the *ABCC6* gene. Research into environmental and genetic modifiers might provide further insights into the unexplained phenotypic variability.

1. Introduction

Pseudoxanthoma elasticum (PXE, OMIM 264800) is a rare autosomal recessive disorder characterized by the fragmentation and calcification of the elastic fibers of the skin, the peripheral arteries and Bruch's membrane in the eyes [1]. In the skin, this results in pseudoxanthomas and severe skin loosening due to reduced elasticity [1]. In the vasculature, it results in peripheral arterial disease (PAD), but gastrointestinal bleeding and microvascular brain damage have also been reported [1–3]. Calcification of Bruch's membrane in the retina results in peau d'orange and angioid streaks. The latter are small fractures in Bruch's membrane, which allow for the ingrowth of choroidal neovascularizations with subsequent exudation, subretinal hemorrhage and scarring. Together with macular atrophy, this causes a high risk of visual

* Corresponding author. Department of Vascular Medicine, University Medical Center Utrecht, PO Box 85500, 3508, GA, Utrecht, the Netherlands.
E-mail address: W.Spiering@umcutrecht.nl (W. Spiering).
[1] These authors contributed equally to this work.
[2] These authors contributed equally to this work.

https://doi.org/10.1016/j.atherosclerosis.2021.03.012
Received 18 January 2021; Received in revised form 26 February 2021; Accepted 10 March 2021
Available online 13 March 2021

impairment in PXE [4].

PXE is caused by pathogenic variants in the *ABCC6* gene, although overlapping phenotypes due to variants in the *ENPP1* and *GGCX* genes have been reported [5]. *ABCC6* encodes the ABCC6 transporter and is mainly expressed in the liver and kidneys [6]. The precise function of ABCC6 and its substrate is not yet fully understood. Low-grade inflammation [7], elastin degradation [8], and the primary deficiency in calcification inhibitors might all underlie the systemic calcification seen in PXE [6]. It has been shown, however, that PXE results in low systemic levels of inorganic pyrophosphate (PPi). PPi is an important inhibitor of calcification and the low levels seen in PXE play a role in the increased multi-organ calcification [6,9].

The phenotype of PXE is highly variable between patients and even within families with the same causative variants [10]. Several studies investigated the association between the different genotypes and the clinical phenotypes to better predict the course of disease in individual patients [11–15]. These studies are complicated by the high number of different *ABCC6* variants since several of the more than 300 variants that cause PXE are unique for different families [11,16]. In addition, due to the rarity of the disease, most studies are hindered by low patient numbers to reach adequate statistical power. One study showed that patients with two loss-of-function variants have an increased risk of developing subretinal hemorrhage or scarring and severe claudication, compared with patients with one or two non-truncating variants [11], but most studies could not find a genotype-phenotype correlation [12,13,15]. Most studies used (a modified version of) the Phenodex classification, which is a composite score of clinical outcomes in organs affected by PXE [12]. Since ectopic calcification underlies these clinical outcomes, measures of ectopic calcification could serve as an intermediate endpoint for clinical outcomes.

To gain better insight into the etiology of PXE and the role of calcification in different organs, we studied the genotypes, calcification measures and clinical phenotypes in the skin, arteries and the eyes in a large cohort of PXE patients. Furthermore, the association between the genotypes and these different phenotypes in PXE were investigated.

2. Patients and methods

2.1. Participants

PXE patients were recruited from the Dutch National Expertise Center for PXE in the University Medical Center Utrecht, the Netherlands. Based on an estimated prevalence of 1:25,000 to 1:50,000 [14,17,18], we assume that 40–90% of the PXE patients in the Netherlands have been seen in our hospital. All patients had a clinical diagnosis of PXE based on the criteria of Plomp *et al.* (2010) [1]. In short, patients had to present with two of the three following criteria: skin involvement (pseudoxanthomas), eye involvement (peau d'orange and/or angioid streaks), or genetic confirmation (biallelic variants in the *ABCC6* gene or a first-degree relative with PXE). For this study, clinical and molecular data (genetics, CT scans, ankle-brachial index after treadmill tests, skin photography, ophthalmological examination and imaging) was used. This cross-sectional study was approved by the medical ethical review board of the University Medical Center Utrecht (IRB# 18-767, 15-446, 19-257). Participants gave written informed consent for the use of their medical files for research purposes.

2.2. Genotyping

Genomic DNA was isolated from whole blood. Specific primers were used to avoid the amplification of *ABCC6* pseudogenes ψ1 and ψ2 [19]. All *ABCC6* exons and the flanking intron sequences were analyzed as part of the genetic screening for regular clinical care. Sanger sequencing was performed to identify single nucleotide polymorphisms (SNPs) and small deletions and insertions, and multiplex ligation-dependent probe amplification (MLPA) was performed to screen for larger deletions in the *ABCC6* gene (reference sequence NM_001171.5, MLPA kit P092B ((https://www.mrcholland.com/)). The pathogenicity of all *ABCC6* variants was estimated based on the Sherloc criteria, a refinement of the guidelines for variant classification of the American College of Medical Genetics and Genomics –Association for Molecular Pathology, and classified as benign (class 1), likely benign (class 2), variant of unknown significance (VUS, class 3), likely pathogenic (class 4) or pathogenic (class 5) [20,21]. Patients with benign and likely benign variants were excluded from the analysis. VUS with a tendency towards benign or pathogenic, as based on the Sherloc criteria, were classified as such. Variants were classified into three groups [1]: truncating variants (nonsense, out-of-frame insertions or deletions, splice site variants that result in a frameshift, and deletions of the whole *ABCC6* gene) [2], non-truncating variants with presumably some residual conservation of the protein function (missense variants, in-frame insertions or deletions and splice site variants that result in the lack of an in-frame exon) and [3] variants in which the effect is not clear. The third group was excluded from all analyses. Patients were grouped as having two truncating variants, a mixed genotype of one truncating and one non-truncating variant, or two non-truncating variants.

2.3. Arterial phenotypes

2.3.1. Arterial calcification

Arterial calcification mass was measured on unenhanced low dose (<3 mSv for a 70 kg adult), whole body CT multi-detector row CT scanners (Siemens or Philips, mAs dependent on body weight, 100 or 120 kVp, slice thickness <1 mm which were resampled to 5 mm slices with 4 mm increment) in the carotid siphon, common carotid artery, coronary arteries, thoracic and abdominal aorta, iliac arteries and the femoral and crural arteries. A peripheral artery score was calculated as the sum of the calcification mass scores in the femoral and crural arteries and a total arterial calcification mass score was calculated as the sum of the mass scores in all different arterial beds. Arterial calcification was defined as hyperdense arterial wall lesions with a density above 130 Hounsfield Units (HU). Calcification mass scores were computed as the product of the volume of the lesion in ml and the mean attenuation in HU.

2.3.2. Ankle-brachial index

The ankle-brachial index (ABI) after treadmill test was used to measure PAD. To calculate the ABI, the systolic blood pressure was measured in the left and right brachial arteries, the tibial posterior arteries and the dorsal pedal arteries. During the treadmill test, patients were encouraged to walk on a treadmill with a 10% slope and a speed of 3.5 km/h for 6 min. Patients who stopped prematurely due to pain (claudication) were encouraged to continue walking as soon as possible. During recovery, the ABI was measured during 10 min in a supine position. The lowest value of these ABI measurements was used as the post-treadmill test ABI. ABI measurements were performed by experienced technicians. PAD was defined as an ABI<0.90.

2.4. Skin phenotype

The presence of pseudoxanthomas was systematically scored by the treating physician in the neck (posterior, lateral, anterior), lower lip, axillas, elbows, umbilicus, and groins. The total number of locations was used as a measure of the extent of the skin involvement.

2.5. Ophthalmological phenotypes

All patients underwent routine ophthalmological examination, including best-corrected visual acuity (BCVA) and indirect ophthalmoscopy. Imaging included macular spectral domain optical coherence tomography (SD-OCT), fundus autofluorescence (FAF), near-infrared reflectance imaging (NIR) (all Spectralis HRA-OCT, Heidelberg

Engineering, Heidelberg, Germany) and color fundus photography (FF 450 plus, Carl Zeiss Meditec AG, Jena, Germany). For this study, the ophthalmological data of the first visit was used.

2.5.1. Length of angioid streaks

Since angioid streaks are assumed to occur in an already calcified area of Bruch's membrane, the length of angioid streaks on 55° NIR imaging was used as a proxy for the extent of Bruch's membrane calcification. The length of the longest angioid streak from the center of the optic disc to the retinal periphery was measured and graded into four zones: zone 1 (<3 mm from the center of the optic disc), zone 2 (3–6 mm), zone 3 (6–9 mm) and zone 4 (>9 mm) (Supplemental Fig. 1). We used five 55° NIR images of the posterior pole and mid-periphery for the grading, and color fundus photography was used for comparison when in doubt. In eyes with extensive macular pathology, grading of angioid streaks was not possible and these were graded as 'not assessable' and excluded from the analysis.

2.5.2. Macular phenotype

The presence of choroidal neovascularizations and the severity of macular atrophy were scored in both eyes by three experienced graders (SR, RvL, JOvN). The presence of (in)active choroidal neovascularizations was based on assessment of SD-OCT, fundus photography and fluorescein- or indocyanine green angiography, if available. The presence of macular atrophy was based on FAF, SD-OCT, color fundus photography and NIR. The largest area of macular atrophy was graded as 'no atrophy', 'mild atrophy' (<twice the area of the optic disc) or 'severe atrophy' (>twice the area of the optic disc). An atrophic zone <0.5 optic disc diameter surrounding an (in)active choroidal neovascularizations was considered to be caused by the choroidal neovascularizations and therefore not classified as macular atrophy. Before 2018, both Snellen charts and Early Treatment of Diabetic Retinopathy Study (ETDRS) charts were used. From 2018 on, only ETDRS charts were used. BCVA was converted to the logarithm of the minimum angle of resolution (logMAR).

2.6. Statistical analysis

Patient characteristics are presented as mean ± standard deviation for normally distributed continuous variables, median (interquartile range (IQR)) for non-parametric distributed continuous variables and number (%) for categorical variables. For the ophthalmological phenotypes, data of the right eye was used for descriptive and regression analyses, and for the latter the left eye was used as a confirmation. If imaging of the right eye was not assessable, the left eye was used.

Regression models were built with genotype as the determinant and calcification and clinical phenotypes as the outcome for all clinically proven PXE patients. Log_{10} transformation was performed on the calcification mass scores. Linear regression models were built for continuous outcomes (calcification mass scores, ABI, BCVA), logistic regression models were used for binary outcomes (the presence of choroidal neovascularizations), ordinal logistic regression models were built for ordinal outcomes (extent of angioid streaks, severity of macular atrophy) and Poisson regression models were built for count data (number of locations of pseudoxanthomas). All models were adjusted for age and sex. The models including arterial calcification mass were additionally adjusted for scanner vendor and differences in settings, since this affects calcification mass scores [22]. As a sensitivity analysis,

Table 1
Patient characteristics.

	All clinically confirmed PXE patients				
	Two truncating variants[1]	Mixed genotype[2]	Two non-truncating variants[3]	$p^{1\ vs.2}$	$p^{1\ vs.3}$
Total, n	**158**	**96**	**18**		
Age	51 [40-60]	54 [41 -61]	47 [44-54]	0.58	0.46
Male sex	55 (35)	36 (38)	5 (28)	0.67	0.54
Vascular, n	**148**	**92**	**18**		
Peripheral arterial calcification					
Prevalence	130 (88)	70 (76)	14 (78)	**0.02**	0.24
Mass score	601 [46-2144]	246 [2-1844]	196 [4-553]	0.11	0.06
Total body arterial calcification					
Prevalence	143 (97)	85 (92)	18 (100)	0.14	0.43
Mass score	1944 [204-59836]	1118 [46-4291]	280 [53-2836]	0.21	0.18
Ankle brachial index	0.90 [0.60–1.03]	0.98 [0.70–1.06]	0.89 [0.69–1.06]	0.07	0.76
Peripheral arterial disease	77 (50)	39 (41)	9 (50)	0.16	0.98
Pseudoxanthomas, n	**154**	**91**	**18**		
Prevalence	137 (89)	82 (90)	17 (94)	0.78	0.47
Number of locations	4 [2-5]	3 [2-5]	3 [2-5]	0.94	0.68
Ophthalmology, n	**156**	**96**	**18**		
Extent of angioid streaks					
Missing	6	5	1		
<3 mm	2 (1)	1 (1)	0 (0)	0.10	0.50
3–6 mm	30 (20)	31 (34)	6 (35)		
6–9 mm	49 (33)	22 (24)	4 (24)		
>9 mm	69 (46)	37 (41)	7 (41)		
choroidal neovascularizations, prevalence	96 (62)	50 (52)	8 (44)	0.14	0.16
Atrophy					
Mild	18 (12)	14 (15)	2 (11)	0.75	0.22
Severe	22 (14)	12 (13)	0 (0)		
Visual acuity, logMAR	0.10 [0.00–0.80]	0.08 [–0.02–0.56]	0.03 [–0.07–0.37]	0.59	0.21

Data is presented as median [IQR] or n (%). Data was analyzed with the Mann-Whitney *U* test or the χ^2 test when appropriate. A *p*-value <0.05 was regarded as statistically significant. LogMAR = Logarithm of the minimum angle of resolution, PAD was defined as an ankle brachial index <0.90.
Data are presented for the right eye, unless imaging could not be assessed, then the left eye was used. The extent of the angioid streaks was measured as the extent of the longest angioid streak from the center of the optic disk on 55° near infrared reflectance (NIR) imaging. One patient did not have 55° NIR imaging, and in 11 patients, severe scarring or atrophy impaired reliable gradin

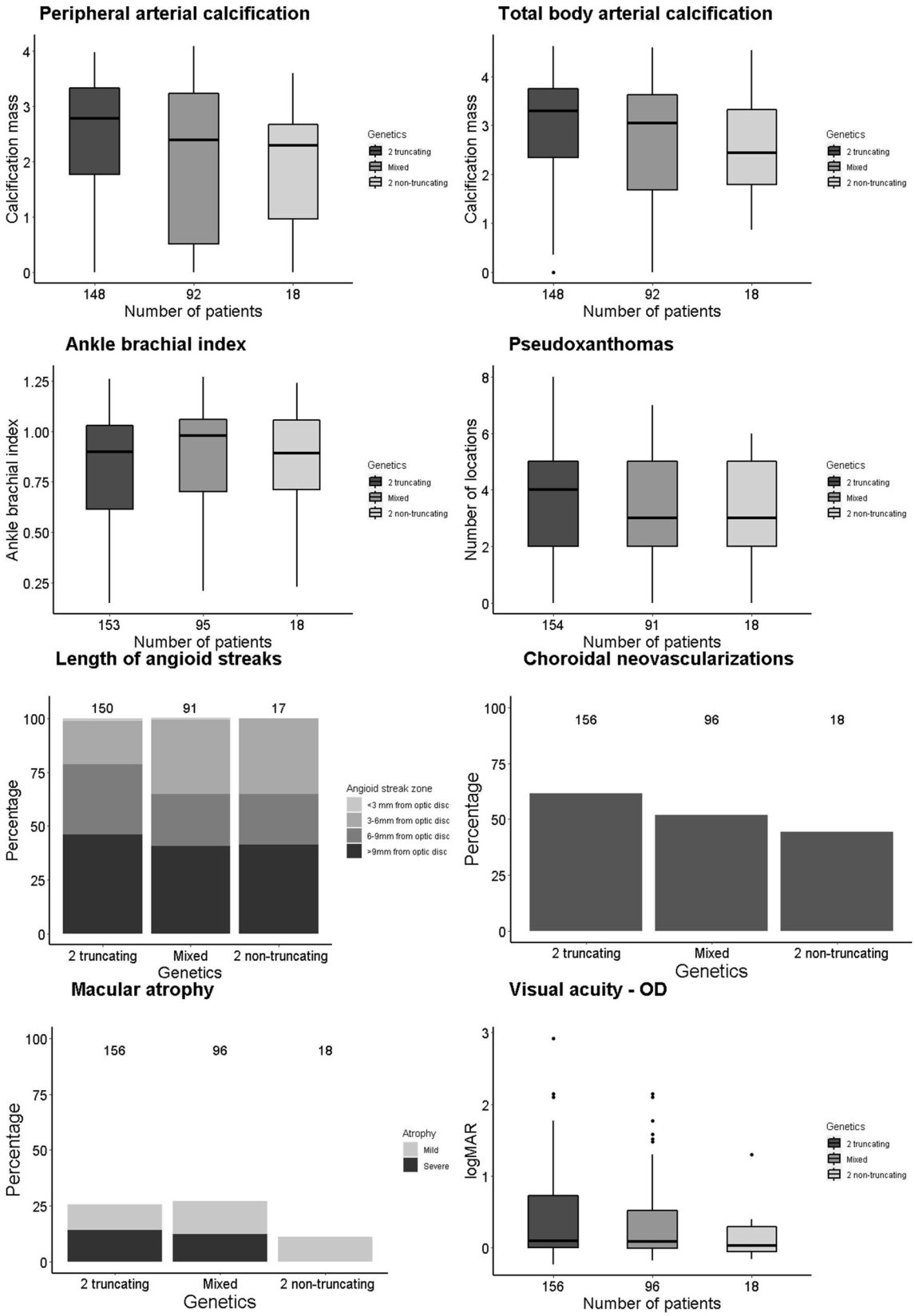

Fig. 1. Correlation between genotypes and different vascular, skin and ophthalmological phenotypes in all clinically confirmed PXE patients.
Patients with two truncating variants have higher arterial calcification mass, lower ankle brachial index, longer angioid streaks and higher prevalence of choroidal neovascularizations than patients with a mixed genotype.

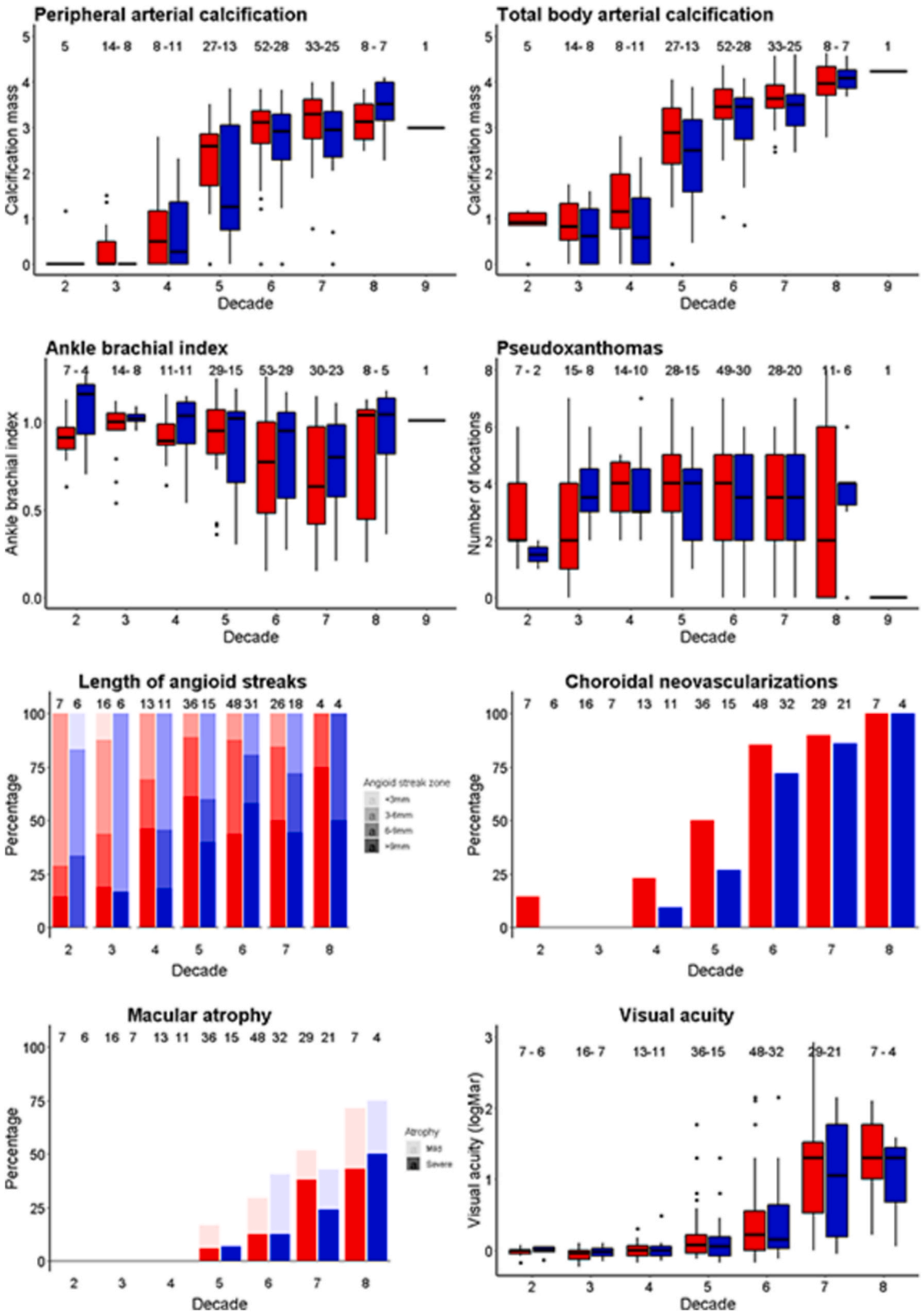

Fig. 2. PXE is a slowly progressive disease.
Except for the number of locations with pseudoxanthomas on the skin, the severity of all phenotypes increases with age in both patients with two truncating variants (red) and patients with a mixed genotype (blue). Data on patients with two non-truncating variants was not shown, since patient numbers were too low to show per decade. For eye data, details of the right eye are shown. (For interpretation of the references to color in this figure legend, the reader is referred to the Web version of this article.)

additional models excluding patients with a VUS were built. The length of angioid streaks mainly varies in patients younger than 50 years and appears static in patients older than 50 years [23]. Therefore, we performed a subgroup analysis in patients younger than 50 years for the length of angioid streaks. Additional models were built excluding patients with two non-truncating variants since this group had very low patient numbers. A p-value <0.05 was regarded statistically significant. All analyses were performed in R studio version 1.1.456. The additional package 'ordinal' (version 2019.12–10) was used to build ordinal logistic regression models.

3. Results

3.1. Participants

In total, 289 clinically confirmed PXE patients were included from 243 families. Genotyping was performed in 282 patients (97%), 273 patients (95%) had a CT scan, 283 patients (98%) had ABI measurements, in 278 patients (96%) the pseudoxanthomas were scored, and 287 patients (99%) had retinal imaging. Of all clinically confirmed PXE patients, 158 (55%) had two truncating variants, 96 (33%) had a mixed genotype, 18 (6%) had two non-truncating variants, 1 (0.3%) had a variant of which the effect was not clear, in 6 patients (2%) only one pathogenic variant was found, and in 2 patients (0.7%) no pathogenic variants were found. One patient (0.3%) had, besides two *ABCC6* variants, a VUS in the *ENPP1* gene, and was therefore excluded from the analyses. In 50 of the 67 homozygous patients (76%), the deletion of the same exon was excluded with MLPA. For the other 17 patients, this data was not available. For an overview of the classification, pathogenicity and frequency of individual variants, see Supplementary Table 1.

3.2. Patient characteristics

The median age at genetic analysis was 51 [IQR, 41-60] years in patients with two truncating variants, 54 [IQR, 41 -61] years ($p = 0.58$ *vs.* two truncating variants) in patients with a mixed genotype, and 47 [44-54] years ($p = 0.46$) in patients with two non-truncating variants. PXE patients with two truncating variants had more often peripheral arterial calcification (88% *vs.* 76%, $p = 0.01$) than patients with a mixed genotype. Although not statistically significant, higher peripheral arterial calcification mass score (601 [46-2144] *vs.* 246 [2-11844], $p = 0.11$), lower ABI (0.90 [0.60–1.03] *vs.* 0.98 [0.69–1.06], $p = 0.07$) and a higher prevalence of choroidal neovascularizations (96 (62%) *vs.* 50 (52%), $p = 0.10$) were found in patients with two truncating variants. The prevalence and number of locations of pseudoxanthomas did not differ between the groups of patients (Table 1). Fig. 1 shows the phenotypes stratified for genotypes. Since PXE is a slowly progressive disease, we also looked at the correlation between phenotype and genotype per decade (Fig. 2). A subgroup analysis excluding patients with a VUS and a subgroup analysis in patients younger than 50 years showed that patients with two truncating variants have longer angioid streaks than patients with a mixed genotype ($p = 0.02$ and $p = 0.04$, respectively) (Supplementary Table 2 and Supplementary Fig. 2). Characteristics of patients with variants in which the effect is not clear and patients with only one or no variants are presented in Supplementary Table 3.

3.3. Genotype-phenotype association

When adjusted for age and sex, there was a significant association between the genotype (two truncating variants, mixed genotype, two non-truncating variants) and peripheral and total arterial calcification mass score (β: -0.25, 95%CI [-0.43; −0.08] and −0.14 [-0.28; −0.00] respectively) and prevalence of choroidal neovascularizations (OR: 0.55, 95% CI [0.31; 0.92]), although these associations attenuated after exclusion of patients with a VUS (Table 2). In younger PXE patients below 50, the genotype was associated with shorter angioid streaks (pOR 0.54, 95%CI [0.30; 0.95]). This association attenuated after exclusion of patients with a VUS. Because of the low number of patients with two non-truncating variants (n = 18), this group was excluded from a subgroup analysis. When adjusted for age and sex, patients with a mixed genotype had significantly lower peripheral and total arterial calcification mass scores (β: -0.39, 95%CI: -0.62; −0.17 and β: -0.28, 95%CI: -0.47; −0.10, respectively), shorter angioid streaks in patients below 50 (pOR: 0.34 [0.15; 0.78]) and a lower prevalence of choroidal neovascularizations (OR: 0.41 95%CI: 0.20; 0.83) compared to patients with two truncating variants. After exclusion of patients with a VUS, these results remained statistically significant for the peripheral and total arterial calcification mass scores and the angioid streaks in younger patients (Table 3).

Table 2
Genotype-phenotype correlation in pseudoxanthoma elasticum. When adjusted for age and sex, PXE patients with two truncating variants have higher arterial calcification mass scores and a higher prevalence of choroidal neovascularization. These association attenuated after exclusion of patients with a variant of unknown significance.

Independent variable: two truncating variants, mixed genotype, two non-truncating variants. Two truncating variants was used as the reference.		
Phenotypes	All clinically confirmed PXE patients	Patients with variant of unknown significance excluded
	Age and sex adjusted model	Age and sex adjusted model
	β/OR/RR [95%CI]	β/OR/RR [95%CI]
Vascular		
Peripheral calcification, mass score, β[a]	−0.25 [-0.43; −0.08]*	−0.16 [-0.34; 0.02]
Total body calcification, mass score, β[a]	−0.14 [-0.28; −0.00]*	−0.10 [-0.25; 0.06]
Ankle brachial index, β[a]	0.03 [-0.02; 0.08]	0.01 [-0.04; 0.07]
Skin		
Pseudoxanthomas, number of locations, RR[b]	0.99 [0.88; 1.10]	1.01 [0.90; 1.13]
Ophthalmology		
Angioid streaks, extending zones, pOR[c]	0.73 [0.50; 1.07]	0.86 [0.56; 1.32]
Angioid streaks, extending zones, pOR[c], younger patients	0.54 [0.30; 0.95]*	0.60 [0.31; 1.11]
Choroidal neovascularizations, presence, OR[d]	0.55 [0.32; 0.92]*	0.64 [0.36; 1.11]
Atrophy, severity, pOR[c]	0.76 [0.45; 1.26]	0.86 [0.49; 1.47]
Visual acuity, β[a]	−0.08 [-0.19; 0.03]	−0.04 [-0.16; 0.08]

Regression models were built with genotype as the determinant and the different phenotypes as the outcome.
[a] Linear regression model (β).
[b] Poisson regression model (rate ratio (RR).
[c] Ordinal regression model (proportional odds ratio (pOR).
[d] logistic regression model (OR). *p-value <0.05.

Table 3
Genotype-phenotype correlation in pseudoxanthoma elasticum in patients with two truncating variants and a mixed genotype. When adjusted for age and sex, PXE patients with two truncating variants have higher arterial calcification mass, longer angioid streaks and a higher prevalence of choroidal neovascularization. After exclusion of patients with a variant of unknown significance, these associations remained significant for the arterial calcification mass scores and the length of angioid streaks in patients below 50 years old.

Independent variable: two truncating variants and mixed genotype. Two truncating variants was used as the reference.		
Phenotypes	All clinically confirmed PXE patients	Patients with variant of unknown significance excluded
	Age and sex adjusted model	Age and sex adjusted model
	β/OR/RR [95%CI]	β/OR/RR [95%CI]
Vascular		
Peripheral calcification, mass score, β[a]	−0.39 [-0.62; −0.17]*	−0.33 [-0.57; −0.09]*
Total body calcification, mass score, β[a]	−0.28 [-0.47; −0.10]*	−0.25 [-0.46; −0.05]*
Ankle brachial index, β [a]	0.06 [-0.01; 0.12]	0.03 [-0.04; 0.11]
Skin		
Pseudoxanthomas, number of locations, RR[b]	1.01 [0.88; 1.17]	1.09 [0.94; 1.26]
Ophthalmology		
Angioid streaks, extending zones, pOR[c]	0.62 [0.37; 1.02]	0.74 [0.43; 1.30]
Angioid streaks, extending zones, pOR[c], younger patients	0.34 [0.15; 0.78]*	0.36 [0.15; 0.83]*
Choroidal neovascularizations, presence, OR[d]	0.41 [0.20; 0.83]*	0.50 [0.23; 1.07]
Atrophy, severity, pOR[c]	0.87 [0.46; 1.64]	1.02 [0.50; 2.03]
Visual acuity, β [a]	−0.07 [-022; 0.07]	0.05 [-0.11; 0.22]

Regression models were built with genotype as the determinant and the different phenotypes as the outcome.
[a] Linear regression model (β).
[b] Poisson regression model (rate ratio (RR).
[c] Ordinal regression model (proportional odds ratio (pOR).
[d] Logistic regression model (OR). * *p*-value <0.05.

4. Discussion

Here we show that PXE patients with a mixed genotype have less severe arterial calcification compared to patients with two truncating variants in the *ABCC6* gene. Especially in PXE patients younger than 50 years, the mixed genotype was associated with shorter angioid streaks as a measure of Bruch's membrane calcification. Although a trend towards lower prevalence of choroidal neovascularizations was seen, we could not confirm an association between the genotype and skin involvement, peripheral arterial disease, choroidal neovascularizations, macular atrophy or visual acuity in our most stringent analyses. Research into other factors, including environmental risk factors and genetic modifiers might provide further insights into the unexplained phenotypic variability and might further improve risk classification in PXE.

A previous study showed that patients with two loss-of-function variants had an increased risk of severe claudication and vascular surgery, and subretinal hemorrhage as measured with the Phenodex classification [11]. Most genotype-phenotype correlation studies in PXE, however, did not find a correlation between the genotype and dermatological, arterial or ophthalmological phenotype [10,12,24–26]. Besides the large heterogeneity in clinical phenotypes [10,12], these studies are typically hindered by lower patient numbers (15-134 patients) due to the rarity of the disease [10,12,24–26]. Even though we included a fairly sized cohort for this disease, we still had borderline statistical power and larger studies might be warranted. Most studies have looked into the correlation between the genotype and clinical outcomes based on the Phenodex classification [12]. This classification includes clinical outcomes in all affected organs in PXE, but does not include direct (semi)quantitative measures of ectopic calcification. Since calcification in the vasculature and Bruch's membrane underlies and probably precedes the clinical consequences of PXE, measures of calcification might provide a better intermediate measure for genotype-phenotype correlation studies and might help with the initial staging of the severity of the disease in these organs.

Approximately 50% of PXE patients in our cohort had PAD, as defined by an ABI below 0.9, which is in line with a previous study [3]. Although the prevalence of PAD was slightly higher in PXE patients with two truncating variants compared to patients with a mixed genotype, this difference was not statistically significant. Previous studies showed that the presence and extent of femoral artery calcification correlates with peripheral arterial disease in PXE [27]. The clear association between genotype and arterial calcification mass in our study suggests that patients with a more severe genotype might suffer from more severe PAD. Larger studies into the correlation between arterial calcification mass and peripheral arterial disease in PXE are awaited.

Since angioid streaks are limited to the area of Bruch's membrane calcification, we used the length of angioid streaks as a proxy for the extent of calcification in Bruch's membrane of the retina. Especially in PXE patients younger than 50 years, two truncating variants increased the risk of longer angioid streaks compared with a mixed genotype. Eventually, choroidal neovascularizations will develop in nearly all PXE patients [28] but they tend to develop earlier in patients with two truncating variants (Fig. 2). Since longer streaks were recently shown to increase the risk for choroidal neovascularizations and macular atrophy, the increased length of angioid streaks at a younger age might underlie the possible association between the genotype and choroidal neovascularizations that we found. Since Bruch's membrane calcification impedes the diffusion of oxygen and nutrients to the outer retina and has an effect on the vitality of the outer retina at a young age, macular atrophy could be considered as the natural endpoint of Bruch's membrane calcification. Macular atrophy might therefore serve as a better clinical endpoint to study Bruch's membrane calcification in PXE [29]. In this study, however, we did not find an increased risk of macular atrophy for more severe genotypes. Probably, environmental risk factors, such as smoking, or genetic modifiers, such as variants of the *VEGF-A* gene are involved in the variability in the ophthalmological phenotype as well [26].

Currently, over 300 different variants in the *ABCC6* gene have been described. The most common variants in our cohort were the truncating p.(Arg1141*) variant, the p.(Trp1259Glyfs*14) and p.(Lys1394Asnfs*9) frameshift variants and the exon 23-29 deletion, which corresponds with previous publications on *ABCC6* variants in PXE [10–12]. However, 51 of the 86 individual variants in our cohort were missense variants. Most of these variants have a low population frequency, or are unique for different families and 19 of these 51 missense variants were classified as a VUS [20]. Since all PXE patients had a confirmed clinical diagnosis, we included patients with a VUS in our primary analysis. Subgroup analysis excluding those patients with a VUS yielded similar point estimates but

resulted in wider confidence intervals and loss of statistical power. Since different missense variants result in proteins with differing residual transporter function or proteins that are retained intracellularly, such variants might still result in a non-functional protein [16]. Variants in arginine are frequent missense variants in our cohort. In general, arginine is important for the protein structure. These variants might therefore have different consequences than others, although we do not see this in our cohort (data not shown). Additional functional analysis of missense variants in the *ABCC6* gene could provide further insight into the unexplained phenotypic variability. The precise function of *ABCC6* is still not clear, but it has been shown that PXE patients have lower systemic levels of PPi [6,9,30]. PPi is an important inhibitor of calcification and the low levels seen in PXE likely play a role in the high calcification propensity in PXE. PPi might therefore be an important biomarker for the severity or predict the progression of PXE. Intraperitoneal PPi supplementation halted calcification in mice and oral PPi increased plasma PPi levels in healthy volunteers [9,31]. In addition, several other therapies that interfere in the PPi homeostasis or ectopic calcification are being developed for PXE and related disorders [32]. Currently, no data on the association between the different genotypes and plasma PPi levels, or the association between plasma PPi and calcification and clinical consequences are available.

A strength of this study is the large amount of multidisciplinary data we collected in a relatively large number of PXE patients. Several limitations of this study have to be addressed. Due to the small number of patients with two non-truncating variants, no conclusions can be drawn for this group. However, since arterial calcification and the prevalence of choroidal neovascularizations in this group was comparable to the group with a mixed genotype, we expect that these patients have a milder phenotype than patients with two truncating variants. Quantification of pseudoxanthomas based on the number of affected locations is a very rough estimate of the skin involvement in PXE. Currently, new in vivo methods to quantify elastin degradation, using two-photon microscopy [33], or calcification of the skin using sodium fluoride PET/CT (NaF-PET/CT) are being developed [34]. Future research might want to look into the genotype-phenotype correlation based on these more sophisticated methods. Since we used data from regular clinical care, there is some heterogeneity in the CT scanner used (Siemens or Philips) and the settings of the scanner (100 or 120 kVp). These differences might have had an effect on the arterial calcification mass scores [22,35]. However, since we adjusted for CT vendor and settings in our regression models, we think it did not affect the findings of this study. The categorical classification of the length of angioid streaks leads to loss of information when compared to a continuous measure. Other approaches, including quantification of Bruch's membrane reflectivity on macular OCT-scan [36] and measurement of the border of peau d'orange on 30° NIR imaging are under development. However, these measurements are only possible in the early stage of disease when there is no macular degeneration yet [36,37]. The length of angioid streaks is the first measure that allows for semi-quantitative measurements in nearly all PXE patients, including those with end-stage disease. In 8 clinically confirmed PXE patients only one or no *ABCC6* variants was found. Since MLPA currently only covers 23 of the 31 coding exons of the *ABCC6* gene, it might be that large deletions in the other eight exons were missed [38]. Since we excluded these patients from our genotype-phenotype analysis, this did not affect our results. Since we did not analyze the *ENPP1* and *GGCX* gene in all patients, we cannot exclude the possibility that there are patients with variants in both *ABCC6* and one of these genes, but since these are all rare diseases the chances are very low. Last, we did not perform segregation analyses in all patients. We therefore cannot prove that the pathogenic variants we found in heterozygous patients were indeed on different alleles.

4.1. Conclusions

In conclusion, we show that PXE patients with a mixed genotype have less severe arterial calcification and length of angioid streaks than PXE patients with two truncating variants in the *ABCC6* gene. Research into the role of PPi, environmental risk factors or modifier genes might provide further insights into the unexplained phenotypic variability and improve risk classification in PXE.

CRediT authorship contribution statement

Jonas W. Bartstra: Conceptualization, Methodology, Investigation, Resources, Data curation, Writing – original draft. **Sara Risseeuw:** Conceptualization, Methodology, Investigation, Resources, Data curation, Writing – original draft. **Pim A. de Jong:** Conceptualization, Methodology, Resources, Writing – original draft. **Bram van Os:** Investigation, Writing – review & editing. **Lianne Kalsbeek:** Investigation, Writing – review & editing. **Chris Mol:** Software, Writing – review & editing. **Annette F. Baas:** Conceptualization, Methodology, Writing – review & editing. **Shana Verschuere:** Methodology, Software, Investigation, Writing – review & editing. **Olivier Vanakker:** Conceptualization, Methodology, Investigation, Writing – review & editing. **Ralph J. Florijn:** Resources, Writing – review & editing. **Jeroen Hendrikse:** Writing – review & editing. **Willem Mali:** Conceptualization, Writing – review & editing. **Saskia Imhof:** Writing – review & editing. **Jeannette Ossewaarde-van Norel:** Conceptualization, Methodology, Investigation, Resources, Writing – review & editing. **Wilko Spiering:** Conceptualization, Methodology, Investigation, Resources, Writing – review & editing.

Declaration of competing interest

The authors declare that they have no known competing financial interests or personal relationships that could have appeared to influence the work reported in this paper.

Acknowledgements

We kindly thank C. Joosten and I. Klaassen (research nurses).

Appendix A. Supplementary data

Supplementary data to this article can be found online at https://doi.org/10.1016/j.atherosclerosis.2021.03.012.

References

[1] A.S. Plomp, J. Toonstra, A.A. Bergen, M.R. van Dijk, P.T. de Jong, Proposal for updating the pseudoxanthoma elasticum classification system and a review of the clinical findings, Am. J. Med. Genet. 152A (2010) 1049–1058.
[2] A.M. Pavlovic, J. Zidverc-Trajkovic, M.M. Milovic, et al., Cerebral small vessel disease in pseudoxanthoma elasticum: three cases, Can. J. Neurol. Sci. J. Canadien des Sci. Neurologiques 32 (2005) 115–118.
[3] G. Leftheriotis, P. Abraham, Y. Le Corre, et al., Relationship between ankle brachial index and arterial remodeling in pseudoxanthoma elasticum, J. Vasc. Surg. 54 (2011) 1390–1394.
[4] S. Risseeuw, J. Ossewaarde-van Norel, C.C.W. Klaver, J.M. Colijn, S.M. Imhof, R. van Leeuwen, Visual acuity in pseudoxanthoma elasticum, Retina 39 (2019) 1580–1587.
[5] Y. Nitschke, G. Baujat, U. Botschen, et al., Generalized arterial calcification of infancy and pseudoxanthoma elasticum can be caused by mutations in either ENPP1 or ABCC6, Am. J. Hum. Genet. 90 (2012) 25–39.
[6] R.S. Jansen, S. Duijst, S. Mahakena, et al., ABCC6-mediated ATP secretion by the liver is the main source of the mineralization inhibitor inorganic pyrophosphate in the systemic circulation-brief report, Arterioscler. Thromb. Vasc. Biol. 34 (2014) 1985–1989.
[7] P.J. Mention, F. Lacoeuille, G. Leftheriotis, L. Martin, L. Omarjee, 18F-Flurodeoxyglucose and 18F-sodium fluoride positron emission tomography/computed tomography imaging of arterial and cutaneous alterations in pseudoxanthoma elasticum, Circ. Cardiovasc. Imaging 11 (2018), e007060.
[8] J.W. Bartstra, W. Spiering, J.M.W. van den Ouweland, W. Mali, R. Janssen, P.A. de Jong, Increased elastin degradation in pseudoxanthoma elasticum is associated with peripheral arterial disease independent of calcification, J. Clin. Med. 9 (2020).
[9] D. Dedinszki, F. Szeri, E. Kozak, et al., Oral administration of pyrophosphate inhibits connective tissue calcification, EMBO Mol. Med. 9 (2017) 1463–1470.

[10] A.S. Plomp, A.A. Bergen, R.J. Florijn, et al., Pseudoxanthoma elasticum: wide phenotypic variation in homozygotes and no signs in heterozygotes for the c.3775delT mutation in ABCC6, Genet. Med. 11 (2009) 852–858.
[11] A. Legrand, L. Cornez, W. Samkari, et al., Mutation spectrum in the ABCC6 gene and genotype-phenotype correlations in a French cohort with pseudoxanthoma elasticum, Genet. Med. 19 (2017) 909–917.
[12] E.G. Pfendner, O.M. Vanakker, S.F. Terry, et al., Mutation detection in the ABCC6 gene and genotype-phenotype analysis in a large international case series affected by pseudoxanthoma elasticum, J. Med. Genet. 44 (2007) 621–628.
[13] A. Iwanaga, Y. Okubo, M. Yozaki, et al., Analysis of clinical symptoms and ABCC6 mutations in 76 Japanese patients with pseudoxanthoma elasticum, J. Dermatol. 44 (2017) 644–650.
[14] N. Chassaing, L. Martin, P. Calvas, M. Le Bert, A. Hovnanian, Pseudoxanthoma elasticum: a clinical, pathophysiological and genetic update including 11 novel ABCC6 mutations, J. Med. Genet. 42 (2005) 881–892.
[15] O. Le Saux, K. Beck, C. Sachsinger, et al., A spectrum of ABCC6 mutations is responsible for pseudoxanthoma elasticum, Am. J. Hum. Genet. 69 (2001) 749–764.
[16] V. Pomozi, C. Brampton, K. Fulop, et al., Analysis of pseudoxanthoma elasticum-causing missense mutants of ABCC6 in vivo; pharmacological correction of the mislocalized proteins, J. Invest. Dermatol. 134 (2014) 946–953.
[17] G. Kranenburg, A.F. Baas, P.A. de Jong, et al., The prevalence of pseudoxanthoma elasticum: revised estimations based on genotyping in a high vascular risk cohort, Eur. J. Med. Genet. 62 (2019) 90–92.
[18] J. Uitto, A. Varadi, L. Bercovitch, P.F. Terry, S.F. Terry, Pseudoxanthoma elasticum: progress in research toward treatment: summary of the 2012 PXE international research meeting, J. Invest. Dermatol. 133 (2013) 1444–1449.
[19] X. Hu, A. Plomp, T. Gorgels, et al., Efficient molecular diagnostic strategy for ABCC6 in pseudoxanthoma elasticum, Genet. Test. 8 (2004) 292–300.
[20] K. Nykamp, M. Anderson, M. Powers, et al., Sherloc: a comprehensive refinement of the ACMG-AMP variant classification criteria, Genet. Med. 19 (2017) 1105–1117.
[21] S. Verschuere, N. Navassiolava, L. Martin, P.I. Nevalainen, P.J. Coucke, O. M. Vanakker, Reassessment of causality of ABCC6 missense variants associated with pseudoxanthoma elasticum based on Sherloc, Genet. Med. 23 (2021) 131–139.
[22] M.J. Willemink, R. Vliegenthart, R.A. Takx, et al., Coronary artery calcification scoring with state-of-the-art CT scanners from different vendors has substantial effect on risk classification, Radiology 273 (2014) 695–702.
[23] S. Risseeuw, J. Ossewaarde-van Norel, C. van Buchem, W. Spiering, S.M. Imhof, R. van Leeuwen, The extent of angioid streaks correlates with macular degeneration in pseudoxanthoma elasticum, Am. J. Ophthalmol. 220 (2020) 82–90.
[24] V. Schulz, D. Hendig, C. Szliska, C. Gotting, K. Kleesiek, Novel mutations in the ABCC6 gene of German patients with pseudoxanthoma elasticum, Hum. Biol. 77 (2005) 367–384.
[25] N. Chassaing, L. Martin, J. Mazereeuw, et al., Novel ABCC6 mutations in pseudoxanthoma elasticum, J. Invest. Dermatol. 122 (2004) 608–613.
[26] E.Y.G. De Vilder, M.J. Hosen, L. Martin, et al., VEGFA variants as prognostic markers for the retinopathy in pseudoxanthoma elasticum, Clin. Genet. 98 (2020) 74–79.
[27] G. Leftheriotis, G. Kauffenstein, J.F. Hamel, et al., The contribution of arterial calcification to peripheral arterial disease in pseudoxanthoma elasticum, PloS One 9 (2014), e96003.
[28] I. Georgalas, D. Papaconstantinou, C. Koutsandrea, et al., Angioid streaks, clinical course, complications, and current therapeutic management, Ther. Clin. Risk Manag. 5 (2009) 81–89.
[29] M. Gliem, P.L. Muller, J. Birtel, D. Hendig, F.G. Holz, P. Charbel Issa, Frequency, phenotypic characteristics and progression of atrophy associated with a diseased Bruch's membrane in pseudoxanthoma elasticum, Invest. Ophthalmol. Vis. Sci. 57 (2016) 3323–3330.
[30] A.M. Sanchez-Tevar, M. Garcia-Fernandez, B. Murcia-Casas, et al., Plasma inorganic pyrophosphate and alkaline phosphatase in patients with pseudoxanthoma elasticum, Ann. Transl. Med. 7 (2019) 798.
[31] V. Pomozi, C.B. Julian, J. Zoll, et al., Dietary pyrophosphate modulates calcification in a mouse model of pseudoxanthoma elasticum: implication for treatment of patients, J. Invest. Dermatol. 139 (2019) 1082–1088.
[32] H. Luo, Q. Li, Y. Cao, J. Uitto, Therapeutics development for pseudoxanthoma elasticum and related ectopic mineralization disorders: update 2020, J. Clin. Med. (2020) 10.
[33] N. Kiss, L. Fesus, S. Bozsanyi, et al., Nonlinear optical microscopy is a novel tool for the analysis of cutaneous alterations in pseudoxanthoma elasticum, Lasers Med. Sci. (2020).
[34] A. Gutierrez-Cardo, E. Lillo, B. Murcia-Casas, et al., Skin and arterial wall deposits of 18F-NaF and severity of disease in patients with pseudoxanthoma elasticum, J. Clin. Med. 9 (2020).
[35] C. Grani, J. Vontobel, D.C. Benz, et al., Ultra-low-dose coronary artery calcium scoring using novel scoring thresholds for low tube voltage protocols-a pilot study, Eur. Heart J. Cardiovasc. Imaging 19 (2018) 1362–1371.
[36] S. Risseeuw, E. Bennink, M.G. Poirot, et al., A reflectivity measure to quantify Bruch's membrane calcification in patients with pseudoxanthoma elasticum using optical coherence tomography, Transl. Vis. Sci. Technol. 9 (2020) 34.
[37] M. Gliem, P.L. Muller, J. Birtel, et al., Quantitative fundus autofluorescence in pseudoxanthoma elasticum, Invest. Ophthalmol. Vis. Sci. 58 (2017) 6159–6165.
[38] A. Legrand, K. Benistan, J.M. Mazzella, et al., Clinical utility gene card: for pseudoxanthoma elasticum, Eur. J. Hum. Genet. 26 (2018) 919–924.